

RECYCLING OF POST SINTERED SANITARYWARE WASTE IN ITS FORMULATION

Mst. Sharmin Mostari, Md. Jahidul Haque

E-Mail Id: mjh.ruet26@gmail.com

Department of Glass & Ceramic Engineering, Rajshahi University of Engineering & Technology (RUET),
Rajshahi, Bangladesh

Abstract- The aim of this work is to minimize the cost of raw materials and to reduce the environmental pollution by recycling the post sintered ceramic sanitaryware waste. Three compositions of ceramic sanitaryware (0% waste, 5% waste, and 10% waste) were prepared by adopting the standard of industrial condition. The sanitary waste was used as a partial replacement of feldspar under three different sintering temperatures (1150 °C, 1175 °C, and 1200 °C). The physical and mechanical properties were analyzed in terms of the variation of composition and temperature. However, the properties of the experimental specimens were improved by the addition of 5% waste, but a significant deterioration of the properties was observed with the further addition of sanitary waste. Moreover, the properties were satisfactory below 1200 °C temperature.

Keywords: Sanitaryware waste, Sintering, Microstructure, Physical analysis, Mechanical analysis.

1. INTRODUCTION

In accordance with the variation of the usages of materials involved in the beneficiation process of ceramic wares, it can be classified into two versatile classes, i.e., the first one involves burned clay products which show red appearance and another one includes commodities showing white manifestation. Conventionally, sanitary ware comes in the second category of this classification with a white appearance, which is composed of clay, quartz, and feldspar [1], [2]. Generally, clay content of this composition contributes to the handling strength of the wares during the green stage of its production, and quartz helps in reducing the shrinkage and the deformation of the fired bodies [3], [4]. In addition to, feldspar promotes the formation of a liquid phase by its fluxing action which allows better densification of the wares.

From the market analysis, it is found that the sanitary ware production rate has achieved an outstanding value of 61.3% in the last two decades all over the world. Particularly in 2014, the total production was 349.3 million pieces worldwide [5]. Along with the development of this sector, a new issue has emerged which is the higher rate of waste disposal from these industries. According to Ana Cecilia, almost 20 to 30 tons of faulty pieces are discarded every month from the sanitary ware industries [6]. The disposal may cause severe problems in the storage, transportation and dumping systems, leading to environmental [7]. It is believed that the recycling of industrial waste is beneficial as it allows the preservation of resources and improves public health and safety [4], [8], [9]. Furthermore, these industrial wastes occupy several unique features including longer endurance, and counteraction capability against degradation; extreme dead heat as well as electrical employment [2].

Several research works were already performed to find out the potential area where the sanitary ware waste could be used as a recycling material. C. Medina proposed to use sanitary waste as a coarse aggregate in concrete to introduce superior mechanical properties (compressive and tensile strength) and to improve its structural sustainability [10]. Later one, reduced moisture expansion with increased bending strength was observed by Muge Tarhan on the usages of sanitary ware waste in porcelain tiles [4]. Furthermore, B. Tarhan used this waste in glazed porcelain tile production where the investigation was satisfactory in terms of the improvement of the technological and mechanical properties.

However, following these explorations, this research was intended to prepare sanitary wares using 5% and 10% sanitary ware waste as a partial replacement of feldspar. To characterize the physical and mechanical properties the analysis was performed at three different densification temperatures (1150 °C, 1175 °C and 1200 °C)

2. METHODOLOGY

2.1 Materials and Methods

All the vitrified sanitary ware samples were prepared under the industrial supervision, comprising of Ball clay, Bijoypur clay, Quartz, Feldspar, and post-sintered sanitaryware waste or pitcher as raw materials. The post sintered sanitary ware waste was used in three different formulations as a replacement of feldspar i.e. CSW0 (0 wt% waste), CSW5 (5 wt% waste) and CSW10 (10 wt% waste) as enlisted in Table-2.1. The raw materials were grounded by jaw crusher (Fritsch PULVERISETTE 1) while the vibratory sieve shaker (Fritsch ANALYSETTE 3) was used to maintain a particular size range of the particles The weighed powders were then ball-milled using water as a milling media with yttria stabilized alumina balls. Then the slurry was dried in an oven (UE600, Memmert, Germany) at 110 °C for 24 h. After re-grounding, the dried powder was compacted into disk pellets

Table-2.1 Designation of Samples

Samples	Batch calculation (wt%)				
	Ball clay	Bijoypur clay	Quartz	Feldspar	PSSWW*
CSW0	10	40	20	30	0
CSW5	10	40	20	25	5
CSW10	10	40	20	20	10

PSSWW* - Post-sintered Sanitary Ware Waste

2.2 Characterization

The chemical composition of the raw constituents was determined through X-ray fluorescence as stereotyped in Table-3.1. The morphologies of the specimens were observed by Scanning Electron Microscope (SEM) (ZEISS EVO-18, UK). Impact strength and compressive strength were measured through Impact Tester (E. J. Payne) and Universal Testing Machine (FS 300 kN, Testometric Co. Ltd. England) respectively. The technological properties, i.e. water absorption, linear firing shrinkage d, apparent density, apparent porosity, loss of ignition) impact strength, compressive strength, Vickers hardness (VH) were analyzed in accordance with the standard of ASTM (American Standard for Testing and Materials).

3. RESULTS AND DISCUSSION

3.1 Chemical Analysis

Table-3.1 Chemical Analysis of Raw Materials

The results of the chemical analysis of the raw materials are tabulated in Table 3.1. From the analysis of the tabulation, it is seen that the SiO₂ content of PSSWW is lower than that of feldspar. However, despite having a

Raw Materials	Chemical Composition (wt%)								
	SiO ₂	Al ₂ O ₃	MgO	TiO ₂	Fe ₂ O ₃	CaO	Na ₂ O	K ₂ O	LOI*
Ball Clay	62.21	21.87	0.84	1.23	3.27	0.33	0.43	2.33	7.28
Bijoypur Clay	48.79	34.16	0.15	0.55	2.28	0.05	0.14	1.99	13.66
Quartz	98.52	0.42	0.04	0.15	0.21	0.00	0.07	0.03	0.03
Feldspar	70.73	17.13	0.11	0.45	0.08	0.71	9.26	0.4	0.25
PSSWW*	68.58	21.96	0.40	0.80	0.78	0.75	3.13	1.22	0.88

LOI* - Loss on Ignition **PSSWW*** - Post-sintered Sanitary Ware Waste

lower quantity of SiO₂, it possesses a higher amount of Al₂O₃ which increases the refractoriness as well as the mechanical properties of the wares by minimizing the residual stresses. Usually, the stress is initiated by the phase transformation of quartz during the densification mechanism which will be further explained in the sintering inspection section [11]. Although the flux Na₂O is lower in PSSWW, other fluxes i.e. MgO, CaO, K₂O are in higher proportion and consequently, these fluxes increase the formation of non-porous and vitreous conformations by diminishing the pores during the densification scheme [12].

3.2 Sintering Inspection

Actually, the following sequential reactions and transformations are performed during the sintering scheme to attain subsequent densification and required properties [13]:

Consideration for the heating cycle,

- $\text{Al}_2\text{O}_3 \cdot 2\text{SiO}_2 \cdot 2\text{H}_2\text{O}$ (Hydroxyl groups of kaolinite) $\xrightarrow{\sim 573^\circ\text{C}}$ $\text{Al}_2\text{O}_3 \cdot 2\text{SiO}_2$ (metakaolin) + 2H₂O ↑
- α - quartz $\xrightarrow{\sim 573^\circ\text{C}}$ β - quartz
- alkali feldspar (sodium: potassium ratio) $\xrightarrow{\sim 700-1000^\circ\text{C}}$ Sanidine (Identical mixed alkali feldspar)
- $3(\text{Al}_2\text{O}_3 \cdot 2\text{SiO}_2)$ (metakaolin) $\xrightarrow{\sim 950-1000^\circ\text{C}}$ $0.282\text{Al}_8(\text{Al}_{13.33}\oplus_{2.66})\text{O}_{32}$ (Spinel structure) + 6SiO₂ (amorphous free)

- $3(\text{Al}_2\text{O}_3 \cdot 2\text{SiO}_2)$ (metakaolin) $\xrightarrow{\sim 950-1000^\circ\text{C}}$ $0.562\text{Al}_8(\text{Al}_{10.67}\oplus_{5.33})\text{O}_{32}$ (Spinel structure) + 3SiO_2 (amorphous free) * \oplus corresponds to vacancy.
- metakaolin $\xrightarrow{\sim 990^\circ\text{C}}$ liberation of amorphous silica
- Potash feldspar + silica $\xrightarrow{\sim 990^\circ\text{C}}$ Eutectic melt and Soda feldspar + silica $\xrightarrow{\sim 1050^\circ\text{C}}$ Eutectic melt
- $0.282\text{Al}_8(\text{Al}_{13.33}\oplus_{2.66})\text{O}_{32}$ (nonequilibrium unstable phase) $\xrightarrow{\sim 1075^\circ\text{C}}$ $3\text{Al}_2\text{O}_3 \cdot 2\text{SiO}_2$ (mullite) + 4SiO_2
- $0.282\text{Al}_8(\text{Al}_{13.33}\oplus_{2.66})\text{O}_{32}$ (nonequilibrium unstable phase) $\xrightarrow{\sim 1075^\circ\text{C}}$ $3\text{Al}_2\text{O}_3 \cdot 2\text{SiO}_2$ (mullite) + 4SiO_2
- Mullite crystals $\xrightarrow{\sim 1200^\circ\text{C}}$ Prismatic crystals
- Consideration for cooling cycles,
- quartz $\xrightarrow{\sim 573^\circ\text{C}}$ quartz particles (volume contraction ~2%)
- β - quartz $\xrightarrow{\sim 225-250^\circ\text{C}}$ β - cristobalite (volume contraction ~5%)

4. MICROSTRUCTURAL ANALYSIS

Fig. 4.1 shows the SEM micrographs of CSW0, CSW5 and CSW10 ceramics sintered at 1150 °C, 1175 °C, and 1200 °C respectively. The establishment of mullite crystals and albite is revealed in the interfaces between the quartz crystals and the glassy phases [4]. At 1150 °C, two types of agglomerates mainly appear, i.e. (i) granular agglomerates (composed of silica and alumina: commonly termed as pure clay relicts) and (ii) higher contrast agglomerates (containing alkaline elements: commonly termed as clay-feldspar relicts) [3].

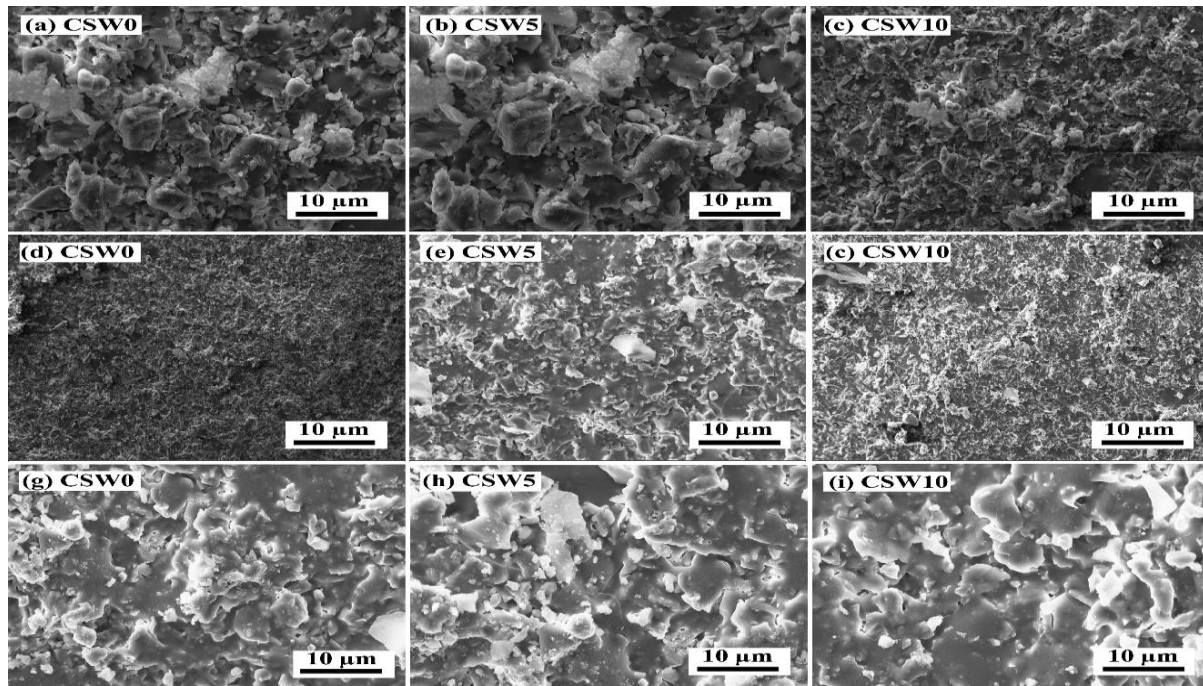


Fig. 4.1 Sem Images OF CSW0, CSW5 AND CSW10 Specimens at a Magnification of 10,000x. PART(a-c), (d-f) AND (g-i) Represent the Samples Sintered at 1150 °C, 1175 °C and 1200 °C Temperature Respectively

Round edges of the quartz particles with surrounding dark rim termed as an amorphous silica solution rim are arisen due to their partial dissolution in the preparatory liquid phase [14], [15]. Micro-cracks among the quartz particles are introduced due to the phase transition between $\alpha \rightarrow \beta$ of quartz particles and also for the relaxation of micro-stresses between the quartz grains and the surrounding glassy phase, which generally arises by the dissimulation of their thermal expansion co-efficient ($\alpha_q \rightarrow 23 \times 10^{-6} \text{ }^\circ\text{C}^{-1}$ and $\alpha_g \rightarrow 3 \times 10^{-6} \text{ }^\circ\text{C}^{-1}$) [16]. At 1175 °C, the feldspar component suffers from reduction behavior accompanied by the formation of newly developed mullite due to the favorable diffusion mechanism [3]. At 1200 °C, mullitisation shows similar characteristics as appeared at 1150 °C. E. Kamseu believed that the addition of catalytic ions i.e. Fe^{3+} and Ti^{4+} enhanced the mullitisation process resulting in enhanced strength [17]. Replacement of Al^{3+} ions with Fe^{3+} from the glass structure during the firing process provides additional support for the formation of mullite resulting in enhanced strength. A variation of the grain size of the quartz crystals is observed and with the addition of CSWW, a decrement pattern of grain size is followed. Microcracking-toughening effect has also arisen whenever the grain size of the quartz particles varies between 25 μm to 50 μm , observed in CSW5 samples sintered at 1175 °C [18].

DOI Number: <https://doi.org/10.30780/IJTRS.V05.I08.004>

pg. 29

www.ijtrs.com

www.ijtrs.org

5. PHYSICAL PROPERTIES

5.1 Water Absorption

According to the ASTM C373-88 standard, each fired sample was dried at 105 °C for 24 h, weighed (D) and subsequently immersed in water. After boiling for 2 h, it is cooled and again weighed (W). Finally, the amount of water absorption by the sample was calculated through the following equation:

$$WA, \% = \left[\frac{(W - D)}{D} \right] \times 100$$

Where D and W are respectively considered as dry weight and saturated weight. It is observed that the amount of water absorption of the samples decreases whenever 5% waste was used. On the other hand, absorption starts to increase while using 10% waste for all the three firing schedules as shown in Fig. 5.1 and it shows similar results up to 5% waste addition as found from the research of Fazilet Gungor [19]. Generally, feldspar enhances the liquid phase formation during firing and causes densification by filling the interconnected pores. But whenever 10% PSSWW is used as a replacement of feldspar, the fluxing reaction is reduced. The increased liquid phase among the narrow channels of the particles provides capillary pressure and causes an improvement of the densification process. Again PSSWW contains Na₂O, K₂O, CaO and Fe₂O₃ which directly affect the sintering parameters i.e. densification rate, eutectic point and crystallization rate [20]. However, with the risen of sintering temperature, the water absorption for CSW0 decreases instead for CSW5 and CSW10 increase.

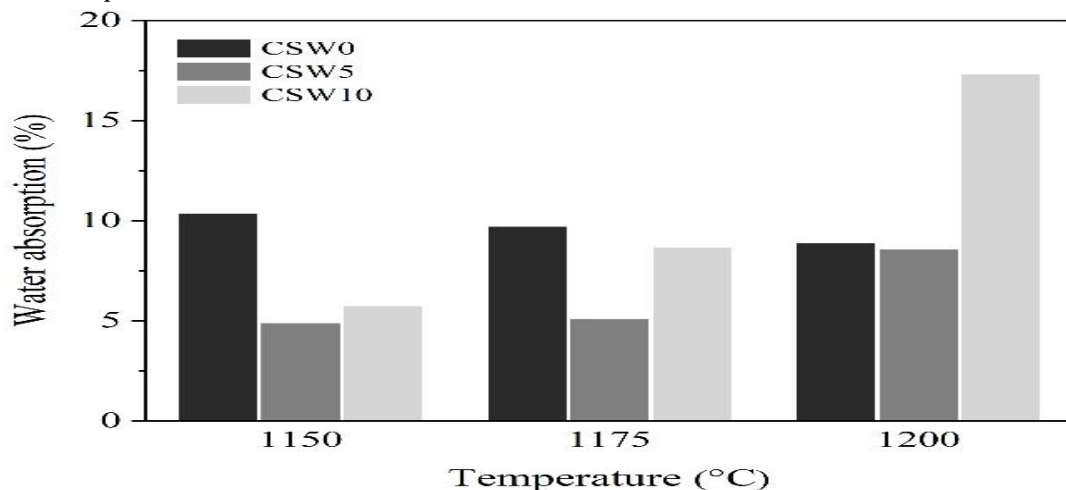


Fig. 5.1 Water Absorption of CSW0, CSW5 and CSW10 Samples as a Function of Firing Temperature

5.2 Bulk Density and Apparent Porosity

According to ASTM D6683-19 Standard Test Method, the bulk density and apparent porosity of the samples were calculated. Maximum density (2.16 g/cm³) is observed for CSW5 at 1150 °C and with the variation of temperature, there is certain reduction in porosity value which is derived from Fig. 5.2. Possible causes for these reduction may be the formation of glassy phase along with the declination of the crystalline phase [17]. From the chemical analysis, it is evident that the entirety of the Fe₂O₃+TiO₂ in PSSWW is 1.58 %. According to Kaushik Dana, these mineralizers influence the sintering scheme by the formation of mullite content [21] as these contents (Ti⁴⁺ and Fe³⁺) change the sintering behavior either by the substitution of Al³⁺ or by their structural unification with the formulated matrix [17].

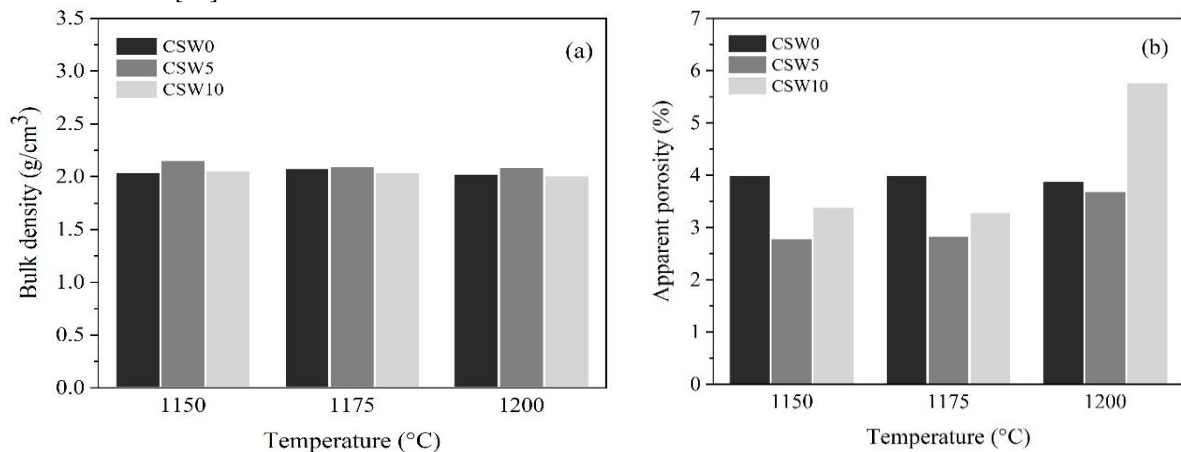


Fig. 5.2 Bulk Density and Apparent Porosity Values of Sanitary Samples with Respect To Temperature

5.3 Linear Shrinkage

The average linear shrinkage, LS (%) values of the representative samples sintered at different temperatures (1150 °C, 1175 °C and 1200 °C) are computed by adopting the following equation according to ASTM C326-82 standard:

$$\text{Linear shrinkage, LS} = \frac{l_1 - l_2}{l_1} \times 100$$

In this equation, l_s denotes the length (mm) of the green body and l_c stands for the length (mm) of the fired body. Fig. 5.3 represents the average shrinkage value of the samples remaining within the acceptable limit (<12%) avoiding the situation of the undesirable deformation [22]. Hither, the minimum shrinkage value is attained from CSW5 formulations which is sintered at 1150 °C. In addition to, the lower scale value is generally associated with the abundance of SiO₂ content [12]. When the temperature rises from 1150 °C to 1175 °C, the specimens show a slight increment of the linear shrinkage value. But at 1200 °C, some unusual values are attained and the backing reason is considered to be over firing [18].

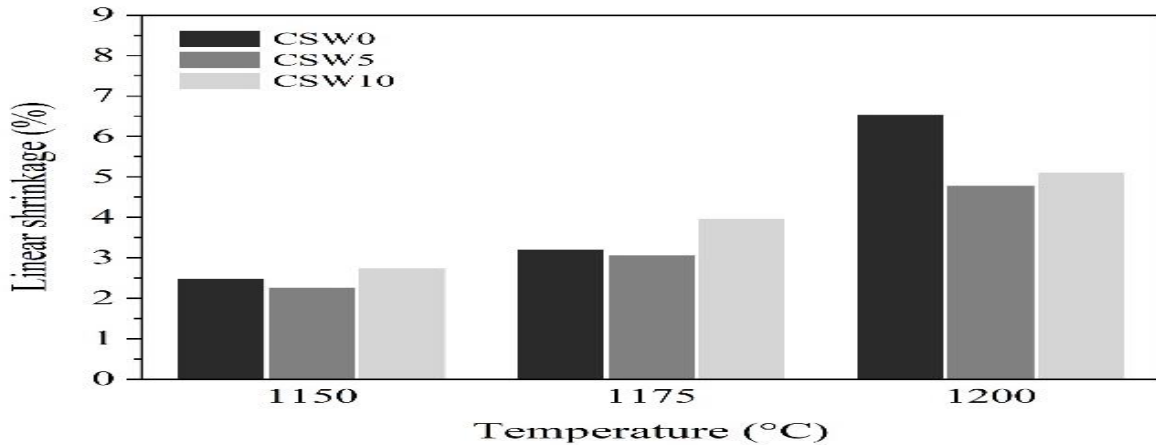


Fig. 5.3 Variation of Linear Shrinkage of the Specimens as a Function of Temperature

5.4 Firing Weight Loss or Loss of Ignition

To determine the weight loss of the ceramic sanitary wares due to the evaporation of the volatile materials, chemically bonded water, organic compounds and carbons, the loss of ignition values are calculated by means of the heading equation maintaining the standard of ASTM D7348-08:

$$\text{Firing weight loss} = \frac{W_1 - W_2}{W_1} \times 100$$

Where, W_1 and W_2 are the weight of the body before and after firing.

Fig. 5.4 shows the loss of ignition curves as a function of temperature. From the results, it is observed that for each firing temperature, there is a decrement in the weight loss on the addition of 5% waste. But, an increment in weight loss is remarked for 10% waste addition.

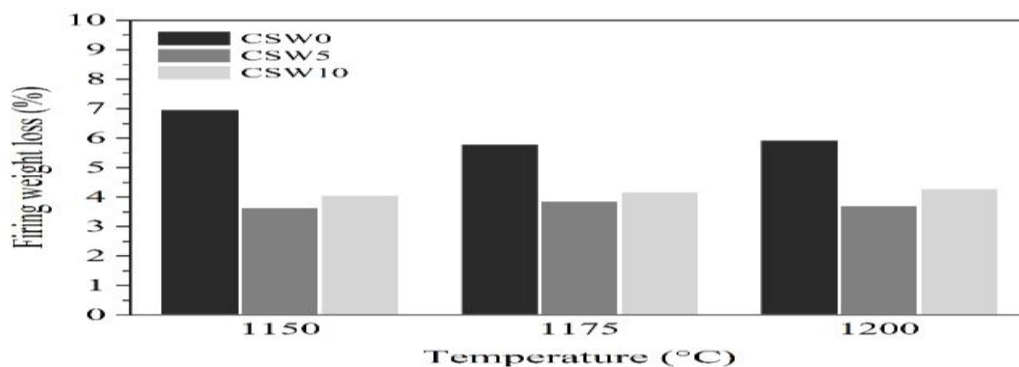


Fig. 5.4 Firing Weight Loss or Loss of Ignition of the Specimens as a Function of Temperature

6. MECHANICAL PROPERTIES

6.1 Impact Strength

To determine the magnitude of a blow that will produce initial failure and the amount of energy necessary to produce complete failure, the impact test on the specimens is performed in accordance with ASTM D256 and the leading equation is employed for further enumeration:

DOI Number: <https://doi.org/10.30780/IJTRS.V05.I08.004>

pg. 31

www.ijtrs.com

www.ijtrs.org

$$\text{Impact strength, } S = \frac{12I}{t^2}$$

Where S is strength factor, t corresponds to the thickness of the sample and I stands for the imposed force.

From the results, it is revealed that the impact strength of samples increases when 5% of waste is used at the firing temperature of 1150 °C and 1175 °C and decreases at 1200 °C. In case of 10% waste, the strength increases gradually with the increasing rate of the firing temperature. But the value of impact strength for similar composition at 1200 °C is abnormal as shown in Fig. 6.1.

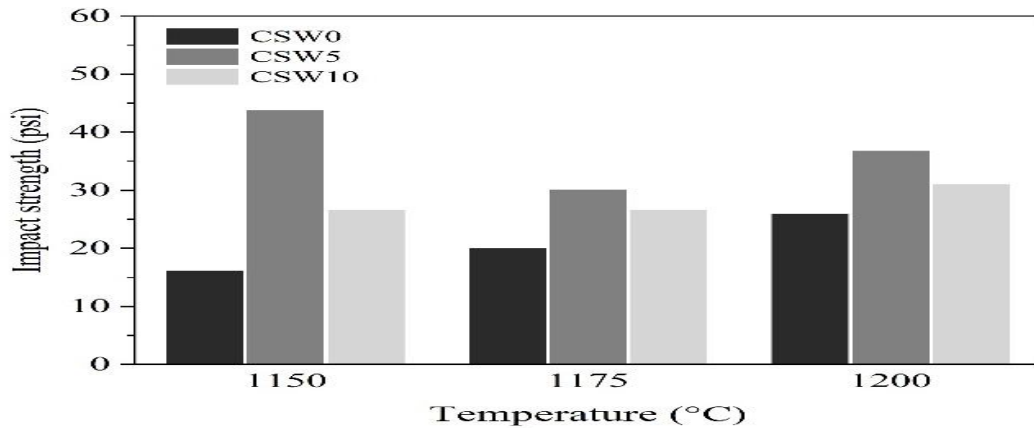


Fig. 6.1 Impact Strength of CSW0, CSW5 and CSW10 Specimens with Respect to the Variation of Densification Temperature

6.2 Compressive Strength

According to ASTM C773-88 standard, the compressive strength of the specimens was determined in conformity with the following formulae to find out the proficiency of them to obstruct the failure under compressive load at room temperature:

$$\text{Compressive strength} = \frac{L}{A}$$

Where L stands for the load applied to the sample and A represents the area of the sample.

From the observation of the computed values of compressive strength as displayed in Fig. 6.2, it is cleared that the maximum value is obtained for 5% waste and further addition results in lessening outcome. Enhanced consolidation with the increment of densification temperature allows the reduction of internal pores as well as the increment of compressive strength.

Generally, there are three basic theories that can explain the strength factors of the experimental samples i.e. Mullite Hypothesis, Matrix Reinforcement Hypothesis, and Dispersion-Strengthening Hypothesis. According to Mullite Hypothesis, the strength increases with the increment of mullite percentage and its interlocking characteristics at higher temperatures. Proceeding to Matrix Reinforcement Hypothesis, the thermal prolongation mismatch inaugurates the thermal compressive stresses and also enhances the strength function. And finally, the last one theory named Dispersion-Strengthening Hypothesis discloses that the enhancement of the strength of the samples is associated with the dispersion of the particles resulting in the limitation of Griffith flaws [13].

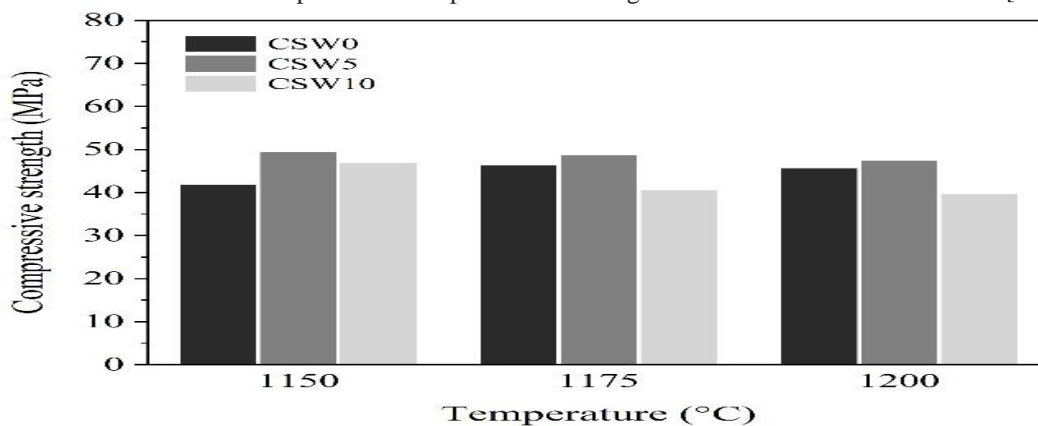


Fig. 6.2 Compressive Strength Vs. Temperature of the Experimental Specimens

CONCLUSION

Based on the results obtained from the exploration of the experimental specimens, the following conclusions can be drawn:

DOI Number: <https://doi.org/10.30780/IJTRS.V05.I08.004>

pg. 32

www.ijtrs.com

www.ijtrs.org

Paper Id: IJTRS-V4-I7-002

Volume V Issue VIII, August 2020

@2017, IJTRS All Right Reserved

- The ceramic sanitary ware waste contains a similar composition of the desired experimental sanitary ware. However, the sanitary ware waste was used as a substitution of feldspar component.
- The results were analyzed at three different sintered temperatures (1150 °C, 1175 °C and 1200 °C).
- The technological and mechanical properties of the fired bodies are mainly manipulated in the presence of mullite and quartz phases which are ensured by SEM.
- The maximum impact strength (43 psi) and compressive strength (49.64 MPa) were obtained by applying 5% waste at a densification temperature of 1150 °C. In addition to, other properties also remained in the considerable limit at this temperature. But for 10% waste incorporation, the properties degrade.
- Mullite Hypothesis, Matrix Reinforcement Hypothesis, and Dispersion-Strengthening Hypothesis mechanisms are the important factors for the enhancement of the mechanical properties.

Finally, it was concluded that post sintering ceramic sanitary ware waste from 0 to 5% was enforceable to use in its composition in case of commercial production and it was better to keep the firing temperature around 1150 °C or as lower as possible.

ACKNOWLEDGMENT

The authors are grateful to Rajshahi University of Engineering & Technology (RUET), Bangladesh for providing the opportunities to perform this research.

REFERENCES

- [1] P. S. S. De Medeiros, H. D. L. Lira, M. A. Rodriguez, R. R. Menezes, G. D. A. Neves, and L. N. D. L. Santana, "Incorporation of quartzite waste in mixtures used to prepare sanitary ware," *J. Mater. Res. Technol.*, vol.8, no.2, pp 2148–2156, 2019.
- [2] A. Halicka, P. Ogrodnik, and B. Zegardlo, "Using ceramic sanitary ware waste as concrete aggregate," *Constr. Build. Mater.*, vol.48, pp 295–305, 2013.
- [3] J. Martín-Márquez, J. M. Rincón, and M. Romero, "Mullite development on firing in porcelain stoneware bodies," *J. Eur. Ceram. Soc.*, vol.30, no.7, pp 1599–1607, 2010.
- [4] B. Tarhan, M. Tarhan, and T. Aydin, "Reusing sanitaryware waste products in glazed porcelain tile production," *Ceram. Int.*, vol.43, no.3, pp 3107–3112, 2017.
- [5] E. Martini, "a Industrial Approach To Ceramics : Sanitaryware an Industrial Approach To Ceramics : Sanitaryware," November 2017, 2018.
- [6] A. C. V. da Nóbrega, R. H. de L. Silva, É. P. Marinho, and M. C. S. de Melo, "Industrial Incorporation of Post Sintering Waste of Ceramic Sanitary Ware in its Own Composition," 2015.
- [7] Z. Bayer Ozturk and E. Eren Gultekin, "Preparation of ceramic wall tiling derived from blast furnace slag," *Ceram. Int.*, vol.41, no.9, pp 12020–12026, 2015.
- [8] F. Andreola, L. Barbieri, I. Lancellotti, C. Leonelli, and T. Manfredini, "Recycling of industrial wastes in ceramic manufacturing: State of art and glass case studies," *Ceram. Int.*, vol.42, no.12, pp 13333–13338, 2016.
- [9] M. Tarhan, B. Tarhan, and T. Aydin, "The effects of fine fire clay sanitaryware wastes on ceramic wall tiles," *Ceram. Int.*, vol.42, no.15, pp 17110–17115, 2016.
- [10] C. Medina, M. I. Sánchez De Rojas, and M. Frías, "Reuse of sanitary ceramic wastes as coarse aggregate in eco-efficient concretes," *Cem. Concr. Compos.*, vol.34, no.1, pp 48–54, 2012.
- [11] N. Marinoni, D. D'Alessio, V. Diella, A. Pavese, and F. Francescon, "Effects of soda-lime-silica waste glass on mullite formation kinetics and micro-structures development in vitreous ceramics," *J. Environ. Manage.*, vol.124, pp 100–107, 2013.
- [12] S. S. Owoeye, B. A. Ajayi, O. E. Isinkaye, and A. Kenneth-Emehige, "Influence of postsintered wastes incorporation on physico-mechanical and structural evolution of vitreous ceramics," *Int. J. Ceram. Eng. Sci.*, vol.1, no.1, pp 42–50, 2019.
- [13] W. M. Cam and U. Senapati, "Porcelain-Raw Materials, Processing, Phase Evolution, and Mechanical Behavior," *J. Am. Ceram. Soc.*, vol.81, no.190529, pp 3–20, 1997.
- [14] J. Martín-Márquez, J. M. Rincón, and M. Romero, "Effect of firing temperature on sintering of porcelain stoneware tiles," *Ceram. Int.*, vol.34, no.8, pp 1867–1873, 2008.
- [15] Y. Iqbal and W. E. Lee, "Fired Porcelain Microstructures Revisited," *J. Am. Ceram. Soc.*, vol.82, no.12, pp 3584–3590, 2004.
- [16] T. Tarvornpanich, G. P. Souza, and W. E. Lee, "Microstructural evolution in clay-based ceramics II: Ternary and quaternary mixtures of clay, flux, and quartz filler," *J. Am. Ceram. Soc.*, vol.91, no.7, pp 2272–2280, 2008.
- [17] E. Kamseu et al., "Characterisation of porcelain compositions using two china clays from Cameroon," *Ceram. Int.*, vol.33, no.5, pp 851–857, 2007.
- [18] C. Leonelli et al., "Enhancing the mechanical properties of porcelain stoneware tiles: A microstructural approach," *J. Eur. Ceram. Soc.*, vol.21, no.6, pp 785–793, 2001.



- I J T R S International Journal of Technical Research & Science**
- [19] F. Gungor, I. Isik, E. Gungor, and E. E. Gültekin, “Usage of ZnO containing wastes in the sanitaryware bodies,” *J. Aust. Ceram. Soc.*, vol.55, no.3, pp 857–863, 2019.
- [20] T. Aydın, N. Kunduracı, and A. Akbay, “The effect of nepheline syenite addition on pyroplastic deformation of sanitarywares,” *Sci. Sinter.*, vol.50, no.1, pp 85–94, 2018.
- [21] K. Dana, S. Das, and S. K. Das, “Effect of substitution of fly ash for quartz in triaxial kaolin-quartz-feldspar system,” *J. Eur. Ceram. Soc.*, vol.24, no.10–11, pp 3169–3175, 2004.
- [22] E. Martini, D. Fortuna, A. Fortuna, G. Rubino, and V. Tagliaferri, “Sanitser, an innovative sanitary ware body, formulated with waste glass and recycled materials,” *Ceramica*, vol.63, no.368, pp 542–548, 2017.